

---

# EFFICIENT GLOBAL ESTIMATION OF CONDITIONAL-VALUE-AT-RISK THROUGH STOCHASTIC KRIGING AND EXTREME VALUE THEORY

---

**Armin Khayer**

Department of Industrial and Systems Engineering  
Auburn University  
Auburn

**Alexander Vinel**

Department of Industrial and Systems Engineering  
Auburn University  
Auburn  
alexander.vinel@auburn.edu

**Joseph J. Kennedy**

Department of Industrial and Systems Engineering  
Auburn University  
Auburn

## ABSTRACT

We consider the problem of evaluating risk for a system that is modeled by a complex stochastic simulation with many possible input parameter values. Two sources of computational burden can be identified: the effort associated with extensive simulation runs required to accurately represent the tail of the loss distribution for each set of parameter values, and the computational cost of evaluating multiple candidate parameter values. The former concern can be addressed by using Extreme Value Theory (EVT) estimations, which specifically concentrate on the tails. Meta-modeling approaches are often used to tackle the latter concern. In this paper, we propose a framework for constructing a particular meta-modeling framework, stochastic kriging, that is based on EVT-based estimation for a class of coherent measures of risk. The proposed approach requires an efficient estimator of the intrinsic variance, and so we derive an EVT-based expression for it. It then allows us to avoid multiple replications of the risk measure in each design point, which was required in similar previously proposed approaches, resulting in a substantial reduction in computational effort. We then perform a case study, outlining promising use cases, and conditions when the EVT-based approach outperforms simpler empirical estimators.

**Keywords** risk measures · Conditional Value-at-Risk · stochastic kriging · metamodeling · simulation

## 1 Introduction

It is often the case that in modeling a stochastic system the decision-maker has no prior knowledge of the response distribution, and instead, through observing the outputs in a simulation or through sampling, they can characterize and quantify its tail behavior, and consequently risk. In many disciplines, minimizing the impact of rare catastrophic losses exceeding a certain threshold is of great importance, and consequently, risk measures designed for quantifying the tail behavior are well-studied in the risk management literature. Conditional Value-at-Risk (CVaR) (which is the main focus of this effort), for instance, a coherent risk measure introduced by R. T. Rockafellar, S. Uryasev (2000), has

gained particular attention as it has been shown to possess significant advantages over other approaches, most notably, Value-at-Risk (P. Krokmal, M. Zabarankin, S. Uryasev, 2011).

It is well known that parametric or non-parametric estimation of the entire density is ill-suited for estimating extreme quantiles of losses. Such methods tend to find a good fit where most of the data falls and ignore the details of the tail behavior. Extreme value theory (EVT), on the other hand, focuses on the extreme outcomes specifically and tries to approximate only the tail distribution, instead of the entire region. This approximation can be valid for any value larger than a certain threshold, and can sometimes be used for regions even outside the range of the observations. EVT is widely used in varied fields, for example, finance or hydrology. While it is also known to improve tail estimates for certain stochastic systems (A. J. McNeil, T. Saladin, 1997), it has not, so far, attracted a sufficient amount of attention in the simulation and stochastic optimization communities. The Peak Over Threshold (POT) is a particular method to model extreme values, which aims to describe the asymptotic tail distribution of a random variable for values above a threshold. It can be demonstrated that the distribution of the values exceeding the threshold can be approximated by a General Pareto Distribution (GPD) for some sufficiently large threshold (A. A. Balkema, L. de Haan, 1974; J. Pickands III, 1975).

In practice, when assessing the risk measures and uncertainty of a stochastic simulation model is of interest, POT is implemented by drawing a large enough sample of the simulation output to ensure that a sufficient number of rare events are observed. Then, the tail behavior is approximated using this sample, and consequently, the risk measures are computed. This is even more computationally expensive when the simulation model covers a wide range of parameters. Moreover, conducting a thorough analysis of the risk measure for every combination of input parameters of the model becomes quickly prohibitive as assessing the risk measure for each requires many function evaluations and replications. This has resulted in significant attention paid to the area of meta-modeling, or surrogate modeling, see R. R. Barton, M. Meckesheimer (2006) for a thorough review.

In this work, we present a metamodeling framework for efficient global prediction of risk across the problem domain. We specifically focus on a particular popular tail measure, Conditional Value-at-Risk (CVaR), and derive the necessary expressions, before expanding it to a more general case of all law-invariant comonotone additive measures of risk. The approach is based on employing a combination of Stochastic kriging and EVT-based estimation of tail behavior, building on the results first discussed in J. J. Kennedy, A. Khayyer, A. Vinel, A. E. Smith (2020) a simple application of EVT as a building block for CVaR estimation in a kriging model was presented.

We expand on the framework in three important ways. First, we present a comprehensive discussion of how EVT methodology can be used for tail estimation, which includes analytical formulae for estimating the variance of CVaR at each design point using POT and the asymptotic properties of the Maximum Likelihood Estimation of the GPD parameters. The estimated variance of the risk measure is subsequently employed within the context of Stochastic kriging as intrinsic noise. This enables the kriging model to more efficiently use the simulation budget without the need for replicating CVaR estimates at each design point to extract an empirical variance estimate, compared to the previously reported results. Second, we expand the definition to the more general case of law-invariant and comonotone additive coherent measures of risk. Finally, we perform more a thorough testing of the approach, comparing it against both the previous version, standard ordinary kriging as well as another specialized approach from the literature.

## 1.1 Brief Review of Related Literature

Building a metamodel for quantile-based risk measures is not a new research avenue. R. Koenker, K. F. Hallock (2001) proposed quantile regression which estimates the conditional median (or other quantiles) of the response variable instead of the conditional mean. In the same direction, S. Dabo-Niang, B. Thiam (2010) proposed a kernel-based statistical estimator for modeling conditional quantiles of spatial processes. M. Liu, J. Staum (2009) proposed a two-level procedure to estimate the expected shortfall (ES) also known as CVaR (note that in this work, we prefer to use the term CVaR, which sometimes is used interchangeably with ES and AVaR, Average Value-at-Risk). Their procedure first constructs a meta-model based on an initial set of design points and then uses the posterior distribution to learn the scenarios that are most likely to entail large losses. It then adds the likeliest points to the design point set and allocates the remaining computational budget accordingly. Another metamodel is constructed at the end of the second stage and is used to estimate CVaR. S. Beguería, S. M. Vicente-Serrano (2006) proposed a procedure based on extreme value analysis and spatial interpolation techniques. The parameters of GPD were regressed over the inputs, resulting in a probability model in which the distribution parameters vary smoothly in space.

M. Reza Najafi, H. Moradkhani (2013) developed a spatial model of the parameters of an extreme distribution (i.e. GPD) through a hierarchical Bayesian process with latent parameters considered as random variables and simulated using Markov Chain Monte Carlo techniques. Various prior distributions are assumed for the GPD parameters and used to assess the sensitivity of the posterior distributions. C. Bracken, K. Holman, B. Rajagopalan, H. Moradkhani

(2018) modeled multivariate nonstationary frequency for hydrologic variables using a Bayesian hierarchical framework. The joint distribution of all variables is modeled by a Gaussian elliptical copula, and it is assumed that the marginal distribution of each variable follows a generalized extreme value (GEV) distribution, where the GEV parameters can vary in time. S. Wang, S. H. Ng (2017) extended the standard stochastic Gaussian process model to the multi-response case to model jointly the quantile (estimated using sectioning) with a correlated and less-noisy expectation to improve the fit and predictions of the quantile metamodel.

X. Chen, K.-K. Kim (2016) extended the stochastic kriging (SK) model to approximate quantiles from stochastic simulation models. The authors analyzed the impact of different non-parametric point and variance estimators of VaR and CVaR such as batching (J. Rougier, 2008), sectioning (S. Asmussen, P. W. Glynn, 2007), sectioning-batching (T. Mitchell, M. Morris, D. Ylvisaker, 1994), and jackknifing (J. H. T. Kim, M. R. Hardy, 2007) on the predictive performance of SK. Furthermore, SK has been shown to be a powerful technique that extends the applicability of deterministic kriging metamodeling to modeling responses from stochastic simulations, including forecasting tail measures (Chen, Kim, 2016). Kennedy et al. (2020) explicitly concentrated on estimating CVaR as the primary measure of risk and tail behavior. POT method was used to estimate CVaR at each design point, while the variance of CVaR was estimated empirically by replicating the POT CVaR estimation.

We discuss specific differences in some of the existing POT- and empirical-based estimation schemes in more detail in Section 3, when presenting the proposed approach. Most importantly, we demonstrate that parametric estimation can be simultaneously accomplished for both risk value and its variance. Specifically, instead of replicating the estimation of CVaR at each design point to estimate its variance, we exploit the asymptotic behavior of the maximum likelihood estimators of the parameters of the GPD to construct an estimate for the variance of CVaR. This then means that a single replication can be sufficient. Consequently, we contribute to the literature on efficiently estimating CVaR by employing a two-stage framework, coupling metamodeling with the parametric estimation of both CVaR and its variance using EVT which distinguishes our effort from the existing literature and more specifically from (Chen, Kim, 2016; Kennedy et al., 2020). Further, we show that in principle any coherent, law-invariant, and comonotonic additive risk measure is amenable to a similar approach, by analyzing the spectral representation of such measures. Note, though, that for any given measure it may be possible to construct a more efficient and straightforward estimator, compared to the generic approach considered here.

## 1.2 Organization

The remainder of this paper is organized as follows. In Section 2, we present an overview of EVT and stochastic kriging, specifically as applied to CVaR. We present the proposed method of estimating CVaR and its variance using EVT in Section 3. Lastly, in Section 4, we present two numerical examples, their experimental designs, and results. We compare the results of our proposed method with that of Kennedy et al. (2020) and Chen, Kim (2016), and we show promising results with the parametric estimation of CVaR and its variance.

## 2 Background

### 2.1 CVaR and its estimation

CVaR is a risk assessment measure that quantifies the amount of tail risk. For a given random variable  $X$ , with its cumulative distribution function (CDF) given by  $F_X$  and its probability density function (PDF) given by  $f_X$ , CVaR at level  $\alpha$  is denoted as  $CVaR_\alpha(X)$ . Recall that the  $\alpha$ -quantile of  $X$  is also known as Value at Risk (VaR):  $q_\alpha = \inf\{x \in R : F_X(x) \geq \alpha\}$ . If the random variable  $X$  is absolutely continuous, CVaR can be defined as the expectation of values exceeding value-at-risk:

$$CVaR_\alpha(X) = E[X|X > q_\alpha] = \frac{1}{1 - \alpha} \int_{q_\alpha}^{+\infty} x f_X(x) dx. \quad (1)$$

For details on the definition in the case of a non-continuous distribution, consider R. T. Rockafellar, S. Uryasev (2002).

Since in practice the CDF,  $F_X$ , is often unknown, an empirical distribution function can be used to describe a sample of observations of variable  $X$ . Consider an i.i.d. sample  $S_t = \{x_1, \dots, x_t\}$  of observations drawn from distribution  $F_X$ . The empirical distribution function is defined as:  $\hat{F}_X^t = t^{-1} \sum_{n=1}^t \mathbb{1}_{\{x_n \leq x\}}$ . Thus the quantile value,  $q_\alpha$ , at level  $\alpha$  can be estimated using the empirical CDF as

$$\hat{q}_\alpha = \inf\{u : \hat{F}(u) \geq \alpha\}$$

leading to the empirical  $CVaR_\alpha(X)$  defined as

$$\widehat{CVaR}_\alpha(X) = \frac{\sum_{i=1}^N x_i \mathbb{1}_{\{x_i \geq \hat{q}_\alpha\}}}{\sum_{i=1}^N \mathbb{1}_{\{x_i \geq \hat{q}_\alpha\}}}. \quad (2)$$

Typical values of  $\alpha$  of interest are usually small (e.g. less than 5%), meaning that empirical CDF, in this case, can be inaccurate. Indeed, small  $\alpha$  leads to few exceedances, and hence, small sample size (and so high variance) for the estimator for VaR and CVaR. Extreme Value Theory (EVT) attempts to approximate CVaR by fitting a model to only the tail of the distribution from scarce samples by exploiting the asymptotic behavior of the tail distribution above a high threshold,  $u$ , and then extrapolating the conditional expectation directly from it. The corresponding exceedance distribution is given by

$$\begin{aligned} F_u(z) &= \mathbb{P}(X - u \leq z | X > u) = \frac{\mathbb{P}(X - u \leq z, X > u)}{\mathbb{P}(X > u)} \\ &= \frac{\mathbb{P}(u < X \leq z + u)}{\mathbb{P}(X > u)} = \frac{F(z + u) - F(u)}{1 - F(u)}, \end{aligned} \quad (3)$$

where the threshold excesses are denoted with  $z$  value and  $F_u$  shows the conditional probability that  $X$  exceeds the threshold,  $u$ , by at most  $z$ . While the distribution function is often unknown, the exceedance distribution can be shown (under some conditions) to be well-described with Generalized Pareto Distribution (GPD) with appropriately selected parameters. GPD with two parameters, shape  $\xi$  and scale  $\beta > 0$ , is a family of continuous probability functions defined by the following cumulative distribution function:

$$G_{\xi, \beta}(x) = \begin{cases} 1 - (1 + \frac{\xi x}{\beta})^{-\frac{1}{\xi}} & \text{if } \xi \neq 0 \\ 1 - e^{-\frac{x}{\beta}} & \text{if } \xi = 0. \end{cases} \quad (4)$$

The following fundamental result characterizes the distribution of exceedances as a GPD.

**Theorem 1 (Balkema, Haan de, 1974; Pickands III, 1975)** Consider a real value  $\xi$  and a random variable  $Y$  and let  $x_0$  be the right endpoint (finite or infinite) of distribution  $F(x)$  and  $0 \leq u < x_0$ . Then a positive measurable function  $\beta(u)$  can be found such that,

$$\lim_{u \rightarrow x_0} \sup_{0 \leq x \leq x_0 - u} |F_u(x) - G_{\xi, \beta(u)}(x)| = 0, \quad (5)$$

if and only if there exist real sequences  $a_n$  and  $b_n$  such that  $F^n(a_n x + b_n) \rightarrow H_\xi(x)$  as  $n \rightarrow \infty$ , for all  $x \in \mathbb{R}$ . Where  $F^n(x) = \mathcal{P}(\max(X_1, \dots, X_n) \leq x)$  denote the cdf of the sample maxima. Note that  $F$  is the CDF of some random variable and  $H_\xi$  is the Generalized Extreme Value (GEV) CDF with parameter  $\xi$ . Then  $F$  belongs to the Maximum Domain of Attraction (MDA) of  $H_\xi$ .

In other words, Theorem 1 states that the distribution of the values exceeding a large enough threshold  $u$  can be approximated by a GPD with shape  $\xi$  and scale  $\beta$  parameters. Note that the inverse of (3) gives the high quantile of the distribution or VaR. For  $\alpha \geq F(u)$ , VaR is given by

$$VaR_\alpha = u + \frac{\beta}{\xi} \left[ \left( \frac{1 - \alpha}{F(u)} \right)^{-\xi} - 1 \right] \quad (6)$$

Consequently, using equation (1), we can estimate the conditional value at risk as:

$$CVaR_\alpha(X) = \hat{q}_\alpha + \frac{\hat{\beta}(u) - \hat{\xi}(\hat{q}_\alpha - u)}{1 - \hat{\xi}},$$

where  $q_\alpha$  is the quantile of confidence level  $\alpha$  of  $X$ ,  $u$  is a sufficiently large threshold such that  $u \leq q_\alpha$ , and  $\hat{\beta}(u)$  is the function used in Theorem 1. This estimation approach is known as Peak Over Threshold-method (POT method) which is one way to model the extreme values. For more details, refer to A. J. McNeil (1997).

L. De Haan, A. Ferreira, A. Ferreira (2006) demonstrated that the exceedances over a given threshold  $u$  are i.i.d and approximately distributed by a GPD. They also showed that the GPD parameters can be estimated using the maximum likelihood estimator (MLE) and proved its asymptotic normality. R. L. Smith (1985) showed that when  $\xi < \frac{1}{2}$ , the

usual properties of consistency, asymptotic normality, and asymptotic efficiency hold for the estimators. MLE estimates can be obtained by solving the following optimization problem

$$(\hat{\xi}, \hat{\beta}) = \underset{\xi, \beta}{\operatorname{argmax}} \sum_{z \in \mathcal{Z}_u} \log g_{\xi, \beta}(z), \quad (7)$$

where  $g_{\xi, \beta}(z)$  is the PDF of the continuous generalized Pareto distribution (GPD) with two parameters  $\xi \in \mathbb{R}$  and  $\beta > 0$ . Using computer simulation, J. R. Hosking, J. R. Wallis (1987) showed that the MLE estimator can exhibit good performance, and such approaches have been used instead for empirical methods in many applications. Note that since the MLE optimization problem does not have a closed-form analytical solution, it must be calculated numerically. It is worth mentioning that, in the context of CVaR estimation with EVT, as long as a suitable threshold is chosen, the MLE estimators are asymptotically normal, but with a biased mean (De Haan et al., 2006). Note that D. Troop, F. Godin, J. Y. Yu (2021) provided a bias correction approach for estimating GPD parameters. As a result, it can be additionally shown that a much lower threshold can be chosen without presenting significant bias if such a corrected approach is employed.

## 2.2 Stochastic kriging

The basic theory of kriging for deterministic modeling was extended to the stochastic modeling setting by B. Ankenman, B. L. Nelson, J. Staum (2010). To accomplish this, both intrinsic and extrinsic uncertainties are considered, where the former characterizes the inherent stochasticity of the simulation model, and the latter is due to the unknown response surface. Let  $X = [x^{(1)}, x^{(2)}, \dots, x^{(k)}]^T$  be a training set, where  $x^{(i)} = [x_1^{(i)}, x_2^{(i)}, \dots, x_d^{(i)}]$ ,  $i = 1, 2, \dots, k$  are  $d$ -dimensional design points, which can be specified using an experiment design. Note that as we are interested in stochastic modeling,  $\bar{Y}^{(i)}$  denotes the average of observations over the entire number of replications at each design point, and the observed response vector for all of the  $k$  design points is  $\bar{Y} = [\bar{Y}^{(1)}, \bar{Y}^{(2)}, \dots, \bar{Y}^{(k)}]^T$ .

Given the notation above, the response value of a stochastic simulation model of replication  $j$  at design point  $x$  can be represented as:

$$y_j(x) = f(x)^T \beta + M(x) + \epsilon_j(x), \quad (8)$$

where  $M(x)$ , a mean zero stationary Gaussian random field (GRF), is referred to as extrinsic uncertainty that represents fluctuations around the trend and exhibits spatial correlation. That is, if two points are spatially located close to each other their value of  $M(x)$  will be similar.  $M$ , defined as a zero mean Gaussian random field, implies that  $M(x^{(1)}), M(x^{(2)}), \dots, M(x^{(k)})$  are multivariate normal for every collection of design points from a discrete domain  $(x^{(1)}, x^{(2)}, \dots, x^{(k)})$ . Therefore,  $M$  can be completely characterized by its covariance matrix. Note that the covariance of the two random variables,  $M(x^i)$  and  $M(x^j)$ , only depends on the distance between  $x^i$  and  $x^j$ .  $\epsilon(x)$  is intrinsic noise. It is assumed that the variance of noise at each design point is not constant and  $\operatorname{Cov}[\epsilon(x), \epsilon(x')] > 0$ . Moreover,  $\epsilon_1(x^i), \epsilon_2(x^i), \dots, \epsilon_{n_i}(x^i)$  are i.i.d. with  $N(0, V(x^i))$  where  $n_i$  shows the number of replications at that design point. Lastly,  $f(x)^T$  is a  $(m \times 1)$  vector of polynomial basis functions.

For a collection of design points  $x^1, x^2, \dots, x^k$ , let  $\Sigma_M(x^i, x^j) = \operatorname{Cov}[M(x^i), M(x^j)]$  be a  $k \times k$  covariance matrix which is obtained by the extrinsic spatial correlation function  $r(x^i, x^j, \theta)$ . Moreover, let  $x_0$  be a new location in the domain and  $\Sigma_M(x_0, \cdot)$  be a  $k \times 1$  vector  $[\operatorname{Cov}[M(x_0), M(x^1)], \operatorname{Cov}[M(x_0), M(x^2)], \dots, \operatorname{Cov}[M(x_0), M(x^k)]]$ . Let  $\Sigma_\epsilon$  be the  $k \times k$  intrinsic covariance matrix. Assuming that  $\beta, \Sigma_M, \Sigma_\epsilon$  are known (Ankenman et al., 2010), the SK predictor is then given as follows:

$$\hat{y}(x_0) = f(x_0)^T \beta + \Sigma_M(x_0, \cdot)^T [\Sigma_M + \Sigma_\epsilon]^{-1} (\bar{Y} - F\beta), \quad (9)$$

where  $F$  is a matrix with its  $i^{\text{th}}$  row given by  $F_i = f(x_i)$ . Assume that  $M(x)$  is second-order stationary, that is, the expectation and variance of  $M(x)$ , respectively  $E[M(x)]$  and  $\operatorname{Var}[M(x)]$ , are constant over the entire study domain, or in other words, they do not depend on the location  $x$  inside the field. Then  $\Sigma_M(x, x')$  can be rewritten as  $\tau^2 r_M(x, x' : \theta)$ . Therefore as mentioned earlier, the covariance between two observations separated by a distance  $h$ ,  $\operatorname{cov}(M(x+h), M(x))$  only depends on the distance  $h$  between the locations and not on the spatial location  $x$  inside the field. Now, let  $R_M(\theta)$  be  $\Sigma_M / (\tau^2)$  then equation (9) can be reformatted as:

$$\hat{y}(x_0) = f(x_0)^T \beta + r(x_0, \cdot) \left[ R_M(\theta) + \frac{\Sigma_\epsilon}{\tau^2} \right]^{-1} (\bar{Y} - F\beta). \quad (10)$$

Note that, when  $\Sigma_\epsilon$  (the intrinsic covariance matrix) is negligible compared to the extrinsic variance, the above equation reduces to the equation of Universal kriging and the model will predict a weighted average of the  $\bar{Y}$  for any given location  $X_0$  which is not in the set of design points. Moreover, if  $\tau^2$  (also known as extrinsic variance) is negligible and

close to zero, then the above equation approaches the polynomial regression  $\widehat{y}(x) = f(x)^T \beta$ , where  $f(x)$  shows the different features of the deterministic regression model. As stated earlier, it is assumed that  $\epsilon_1(x_i), \epsilon_2(x_i), \dots, \epsilon_n(x_i)$  are i.i.d and normally distributed  $\mathcal{N}(0, V(x_i))$ . This assumption can often be justified since the output of a complex simulation model is itself the average of many basic random variables. It is demonstrated that  $V(x_i)$  can be estimated using the following equation,

$$\widehat{V}(x_i) = \frac{1}{n_i - 1} \sum_{j=1}^{n_i} (y_j(x_i) - \bar{Y}(x_i))^2. \quad (11)$$

Assuming  $\Sigma_\epsilon$  is known and equal to  $Diag\{V_1, V_2, \dots, V_k\}$  where  $V_i = \widehat{V}(x_i)/n_i$ ,  $n_i$  gives the number of replications at design point  $x_i$ , and considering the normality assumptions of the kriging predictor, the log-likelihood function of the collected data is (Ankenman et al., 2010):

$$\ell(\beta, \theta, \tau^2) = -\ln[(2\pi)^{\frac{k}{2}}] - \frac{1}{2} \ln[|\tau^2 R_M(\theta) + \Sigma_\epsilon|] - 1/2(\bar{Y} - F\beta)^T [\tau^2 R_M(\theta) + \Sigma_\epsilon]^{-1} (\bar{Y} - F\beta). \quad (12)$$

Since  $R$  may be nearly singular and  $\tau^2$  may be small, maximization over the three parameters simultaneously is unstable (K.-T. Fang, R. Li, A. Sudjianto, 2005). It is demonstrated in practice that the maximum likelihood estimator of  $\beta$  is asymptotically independent of  $(\tau^2, \theta)$  (refer to Fang et al., 2005, for more details). Therefore, one can separately and iteratively estimate  $\beta$  and  $(\tau^2, \theta)$ . Note that unlike  $\beta$  and  $\tau^2$ ,  $\theta$  does not have a closed-form estimator and it requires a numerical search algorithm to maximize the likelihood with respect to  $\theta$ . It is worth mentioning that since  $\Sigma_\epsilon$  is not a function of the parameters, adding the diagonal intrinsic noise matrix,  $\Sigma_\epsilon$ , to the extrinsic covariance matrix,  $\Sigma_M$ , works in our favor, as it makes  $\Sigma = \Sigma_M + \Sigma_\epsilon$  resistant to becoming singular. This may allow maximizing the likelihood function simultaneously over the parameters of the kernel,  $\theta$ , the extrinsic variance of the GRF,  $\tau^2$ , and finally the coefficients of the deterministic trend,  $\beta$ .

### 3 Methodology

#### 3.1 Overall framework

In a risk-driven stochastic simulation system, the decision-makers are interested in describing tail behavior for the underlying distributions of the outputs of the simulation model. Depending on the distribution, which is unknown in most cases, characterizing risk requires many function evaluations at each combination of the input parameters of the system. The idea in this work is to construct a metamodel that can be used globally across the domain of the simulation model, allowing estimation of the risk measure (i.e. CVaR) for any given input in real-time. This task is otherwise computationally expensive if the simulation model itself is used to estimate risk measures for any input, as it requires many observations at each point.

The overall metamodeling framework (Figure 1) consists of two major components, namely risk estimation and construction of a global predictor. The first step in the risk estimation phase is to sample a collection of design points. For each point in this set, the simulation response is observed multiple times to enable estimation of the risk measure, CVaR, using POT. Note that in addition to the POT estimate, CVaR value can also be estimated empirically, i.e. as the average of exceedances, equation (2), similar to Chen, Kim (2016). The estimate of CVaR is highly dependent on the underlying distribution and the samples. Therefore this estimate varies as the samples drawn from the simulation change. In this work, we capture this variability at each design point via the intrinsic noise in SK. Previously, to construct the global surrogate SK model, Chen, Kim (2016) estimated CVaR and its variance empirically. Note that equation (2) can be rewritten as:

$$\widehat{CVaR}_\alpha(X) = \widehat{VaR}_\alpha + \frac{1}{n(1-\alpha)} \sum_{i=1}^n (X_i - \widehat{VaR}_\alpha)^+. \quad (13)$$

Therefore, an estimator of variance (A. A. Trindade, S. Uryasev, A. Shapiro, G. Zrazhevsky, 2007) can be constructed as

$$\widehat{V} = \frac{1}{n(n-1)} \sum_{i=1}^n (W_i - \bar{W})^2, \quad (14)$$

where  $W_i = \widehat{VaR}_\alpha + \frac{1}{1-\alpha} (X_i - \widehat{VaR}_\alpha)^+$  and  $\bar{W} = \frac{1}{n} \sum_{i=1}^n W_i$  is equivalent to  $\widehat{CVaR}_\alpha$ .

In Kennedy et al. (2020) the authors first considered the same approach of estimating CVaR using the POT, however, the variance of CVaR (i.e. expectation of the squared deviation of CVaR observations from its mean) was computed by replicating the estimation of CVaR multiple times at each design point (11).

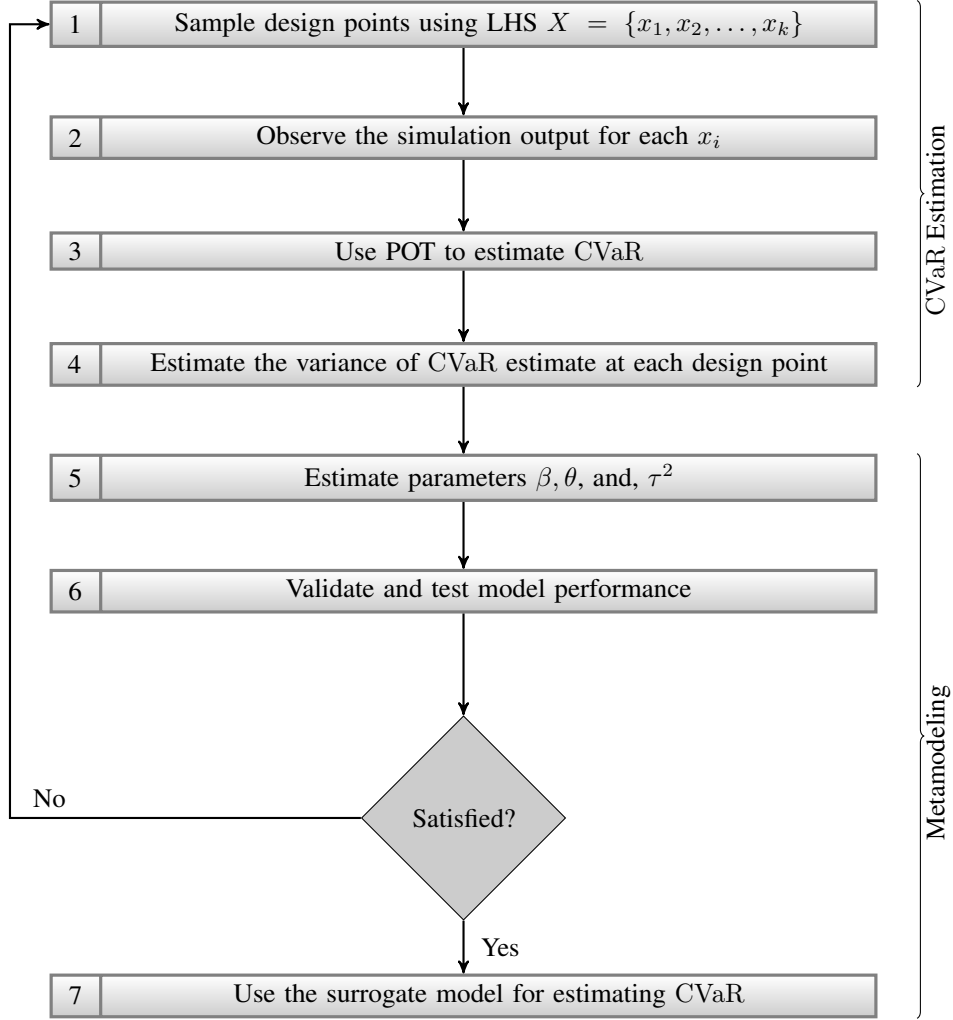


Figure 1: Overall metamodeling framework

In this work, we propose an estimator for the variance of CVaR that directly uses EVT. Compared to Kennedy et al. (2020), this reduces the computational effort by the factor of  $n$ , where  $n$  is the number of replications at each design point (refer to Table 3). Furthermore, it provides a fair comparison between the parametric and non-parametric estimation of CVaR and its variance, and consequently, the performance of the SK model obtained using the POT or empirical CVaR estimation. The next subsection details the proposed approach.

### 3.2 POT-based estimation of CVaR variance

Recall that we use MLE method to estimate the GPD parameters  $\hat{\xi}, \hat{\beta}$ . Given the parameter values, we then obtain a Gaussian asymptotic confidence interval for CVaR at each design point based on equation (15). D. Troop, F. Godin, J. Y. Yu (2019) first proposed an approximate asymptotic confidence interval for the CVaR estimate. Assuming that the approximation of the tail distribution by a GPD is exact, using the delta method, the variance of  $CVaR_\alpha(X)$  is given by

$$\hat{V}[h(\xi, \beta)] \approx \frac{1}{N_u} \left[ \nabla h(\hat{\xi}, \hat{\beta}) \right]^T \mathcal{I}^{-1} \left[ \nabla h(\hat{\xi}, \hat{\beta}) \right], \quad (15)$$

where  $N_u$  is the number of exceedances,  $\mathcal{I}^{-1}$  is the inverse of the Fisher information matrix, and  $\nabla h(\xi, \beta)$  is the column vector representing the gradients of  $h$ , i.e.,

$$h(\xi, \beta) = q + \frac{\beta - \xi(q - u)}{1 - \xi}.$$

The partial derivative of  $h(\xi, \beta)$  can then be obtained as

$$\frac{\partial h(\xi, \beta)}{\partial \xi} = \frac{q - u + \beta}{(1 - \xi)^2}, \quad \frac{\partial h(\xi, \beta)}{\partial \beta} = \frac{1}{1 - \xi}.$$

Consequently, the Fisher information matrix (see Troop et al., 2019, for more details) then can be evaluated as follows:

$$\mathcal{I} \equiv -\mathbb{E} \begin{bmatrix} \frac{\partial^2 \log g_{\xi, \beta}(Z)}{\partial \xi^2} & \frac{\partial^2 \log g_{\xi, \beta}(Z)}{\partial \xi \partial \beta} \\ \frac{\partial^2 \log g_{\xi, \beta}(Z)}{\partial \xi \partial \beta} & \frac{\partial^2 \log g_{\xi, \beta}(Z)}{\partial \beta^2} \end{bmatrix} \approx -\frac{1}{N_u} \sum_{j=1}^{N_u} \begin{bmatrix} \frac{\partial^2 \log g_{\xi, \beta}(z_j)}{\partial \xi^2} & \frac{\partial^2 \log g_{\xi, \beta}(z_j)}{\partial \xi \partial \beta} \\ \frac{\partial^2 \log g_{\xi, \beta}(z_j)}{\partial \xi \partial \beta} & \frac{\partial^2 \log g_{\xi, \beta}(z_j)}{\partial \beta^2} \end{bmatrix}, \quad (16)$$

where  $Z$  is a random variable with a  $GPD(\xi, \beta)$  distribution.

We can then find partial derivatives from the information matrix for the case  $\xi \neq 0$  as,

$$\begin{aligned} \frac{\partial}{\partial \beta} \log g_{\xi, \beta}(z) &= \frac{1}{\beta} \left[ \frac{z(\xi + 1)}{\beta + \xi z} - 1 \right] \\ \frac{\partial}{\partial \xi} \log g_{\xi, \beta}(z) &= \frac{1}{\xi^2} \log \left( 1 + \frac{\xi z}{\beta} \right) - \left( \frac{1}{\xi} + 1 \right) \frac{z}{\beta + \xi z} \\ \frac{\partial^2}{\partial \beta^2} \log g_{\xi, \beta}(z) &= -\frac{1}{\beta^2} \left[ \frac{z(\xi + 1)}{\beta + \xi z} - 1 \right] - \left[ \frac{z(\xi + 1)}{\beta(\beta + \xi z)^2} \right] \\ \frac{\partial^2}{\partial \beta \partial \xi} \log g_{\xi, \beta}(z) &= \frac{1}{\beta} \left[ \frac{z}{\beta + \xi z} - \frac{z^2(\xi + 1)}{(\beta + \xi z)^2} \right] \\ \frac{\partial^2}{\partial \xi^2} \log g_{\xi, \beta}(z) &= -\frac{2}{\xi^3} \log \left( 1 + \frac{\xi z}{\beta} \right) + \frac{2}{\xi^2} \frac{z}{\beta + \xi z} + \left( \frac{1}{\xi} + 1 \right) \frac{z^2}{(\beta + \xi z)^2}. \end{aligned}$$

Putting it all together, equation (15) then provides the desired estimate for variance of CVaR.

Once a sample of observations is drawn for each design point, using the definitions, CVaR and the estimate of the variance of CVaR can be calculated. Further, the set of the locations of the design points, the estimated CVaR, and its variance at each design point ( $x^{[i]}$ ,  $CVaR_{\alpha}^{[i]}$ ,  $\widehat{V}^{[i]}$ ) are used to construct the SK model. Table 1 summarizes the three different approaches to estimating the variance of CVaR at each design point, where we outline the main characteristics, the corresponding equation, and whether it applies to the empirical or POT estimate of CVaR itself.

Method	Equation	Comments	Estimate of CVaR
Expectation of the squared deviation	(11)	used in Kennedy et al. (2020)	POT or empirical
Empirical	(14)	first proposed by (Trindade et al., 2007) and used in (Chen, Kim, 2016)	empirical
Approximate asymptotic variance	(15)	proposed in general in Troop et al. (2019). We propose to use this estimate in SK as an intrinsic variance estimate	POT

Table 1: Summary of the methods for estimating the variance of CVaR at each design point

In the metamodeling phase, the first step is estimating the parameters of the metamodel by maximizing the likelihood function (12) simultaneously over the parameters of the kernel. The metamodel is then validated over the test set. If the performance is satisfactory, the model can be used globally over the domain to quantify the risk measure at any location. If the performance is not satisfactory, the whole process can be repeated, or a larger number of design points can be used to improve the overall performance of the metamodel.

### 3.3 Generalization to other coherent measures of risk

While the derivation above is explicitly constructed for CVaR, it can be observed that, in principle, similar construction is possible for any coherent measure of risk subject to some non-restrictive assumptions. To that end, recall that C. Acerbi (2002) proposed the following spectral representation for a coherent measure of risk,

$$\mathcal{R}(X) = \int_0^1 VaR_{\lambda}(X) \phi(\lambda) d\lambda, \quad (17)$$



where  $\phi$  is an admissible risk spectrum, i.e.,  $\phi \in \mathcal{L}^1([0, 1])$  is positive, non-decreasing, and integrating to 1. It can further be shown that this representation is complete for the set of coherent measures of risk that are also law-invariant and comonotonic additive, see also S. Kusuoka (2001) for more details.

Note that while not all coherent measures of risk are law-invariant and/or comonotone additive, the two properties are natural for most practical use cases. Law-invariance requires the risk measure to give the same value of risk for all random variables that have the same distribution. Recall that two random variables  $X$  and  $Y$  are comonotone, if there exist increasing real functions  $f$  and  $g$  and another random variable  $Z$ , such that  $X = f(Z)$  and  $Y = g(Z)$ . This implies that the two cannot serve as a hedge to each other, and therefore, a risk measure can be expected to be comonotone additive, since risk should not be reduced by combining two comonotone outcomes together, as no diversification is possible. Consequently, both properties are often considered essential for any practical measure of risk. In other words, coherent measures of risk that allow for the spectral representation above span all risk measures of practical interest. See Krokmal et al. (2011) and references therein for more details on the interpretation of these and other properties of risk measures.

Using equation (6),  $VaR_\alpha(X)$  can be replaced with its closed-form formula. Therefore, we can estimate the coherent risk measure using POT for any  $\phi$  as follows.

$$\mathcal{R}(X) \approx h(\xi, \beta) = \int_0^1 \left( u + \frac{\beta}{\xi} \left[ \left( \frac{\lambda}{F(u)} \right)^{-\xi} - 1 \right] \right) \phi(\lambda) \, d\lambda \quad (18)$$

$$= u - \frac{\beta}{\xi} + \frac{\beta F(u)^\xi}{\xi} \int_0^1 (\lambda)^{-\xi} \phi(\lambda) \, d\lambda. \quad (19)$$

Note that in general, the above integral can be improper at the lower boundary, however, for a proper risk measure the integral will always be well-defined and finite Acerbi (2002). For instance, for the case of CVaR,

$$CVaR_\alpha(X) = \frac{1}{1-\alpha} \int_\alpha^1 VaR_\lambda \, d\lambda. \quad (20)$$

Following an analogous approach to (Troop et al., 2019), we can estimate the variance of any coherent risk measure achieved from equation (17). To do so, the  $\nabla h(\xi, \beta)$  which is the column vector representing the gradients of  $h(\xi, \beta)$ , should be derived. While an analytical expression may not be possible to obtain in general, for any given measure, i.e., any given function  $\phi$ , such a derivation can follow the same approach as presented in the previous section in the case of CVaR. Even if such a derivation is not possible, equation (19) can be differentiated numerically to produce the required estimates.

It is also worth noting that, while this discussion provides a pathway to estimate variance for (law-invariant and comonotone additive) coherent measures of risk in general, for any particular measure of interest a more computationally efficient approach may be possible, depending on how the measure is defined. For example, consider the Higher-Moment Coherent Measure of Risk (HMCR), proposed in P. A. Krokmal (2007), which generalizes CVaR. One way to define it is by solving equation

$$(1-\alpha)^{-1/(1-p)} = \frac{\left\| (X - \eta_{p,\alpha}(X))^+ \right\|_p}{\left\| (X - \eta_{p,\alpha}(X))^+ \right\|_{p-1}}, \quad p > 1. \quad (21)$$

Its solution  $\eta_{p,\alpha}(X)$  plays the role of VaR in CVaR definition, so, for example, Second-Moment Coherent Measure of Risk (SMCR) is given as

$$SMCR_\alpha(X) = \eta_{2,\alpha}(X) + (1-\alpha)^{-2} \left\| (X - \eta_{2,\alpha}(X))^+ \right\|_1 \quad (22)$$

$$= \eta_{2,\alpha}(X) + (1-\alpha)^{-2} E(X - \eta_{2,\alpha}(X))^+ \quad (23)$$

This expression then can be used directly in the same way as the VaR-based definition of CVaR to construct POT estimate.

## 4 Experiments and Results

### 4.1 Experimental Design

We develop two test cases to demonstrate our methodology's capabilities. The first case, similar to (Kennedy et al., 2020), involves a benchmark function studied in three scenarios, introducing different random noise types (triangular,

Pareto, normal distributions) to create a complex surface affecting CVaR estimation. The second case, inspired by Chen, Kim (2016), uses a stochastic activity network to illustrate practical application in a complex simulation model.

The first test case is a widely-used two-dimensional function, given as  $f_i(x_1, x_2) = x_1 \sin(\pi x_2) + x_2 \sin(\pi x_1) + \epsilon_i(x_1, x_2)$ , where  $\epsilon_i(x_1, x_2)$  is random noise and  $x_1, x_2 \in [-\pi, \pi]$ . The random noise is studied under three different scenarios as described in Table 2. The function, as well as true CVaR values, are as discussed in detail in M. Norton, V. Khokhlov, S. Uryasev (2019). The True CVaR column in Table 2, shows the analytical closed-form formula for computing CVaR under the three different scenarios.

Table 2: Additive noise terms and expressions for calculating the true CVaR values analytically

Scenario Description	$\epsilon_i(x_1, x_2)$	True CVaR [ $\epsilon_i(x_1, x_2)$ ]
normal (thin) tail	$N(\mu = 0, \sigma = \sqrt{(x_1^2 + x_2^2)})$	$\frac{\sqrt{(x_1^2 + x_2^2)} \phi(\Phi^{-1}(\alpha))}{\alpha}$
finite tail	$Triangular(\min = 0, \max = \sqrt{(x_1^2 + x_2^2)})$	$\sqrt{(x_1^2 + x_2^2)} \left(1 - \frac{\sqrt{2(1-\alpha)}}{3}\right)$
heavy tail	$Pareto(a = 2, x_m = 2 + \sqrt{(x_1^2 + x_2^2)})$	$\frac{2(2 + \sqrt{(x_1^2 + x_2^2)})}{(1-\alpha)^{1/2}}$

Multiple observations of the simulation response at each design point are required (denoted by  $N$  in this work) to estimate CVaR. Moreover, to empirically evaluate the intrinsic variance using equation (11), it is required to replicate the estimation of CVaR. The number of replications at each design point is denoted by  $n$ . Note that the proposed approach does not require multiple replications. Finally, the SK model is constructed by sampling observations from  $K$  design points. Experimental trials are designed to assess the effects of the different components of this framework over the final performance of the metamodel for different combinations of  $N, k, n$ . Table 3 presents the different scenarios and computational budget levels. Naturally, the total computational budget (measured in the number of evaluations) can be calculated as  $N \times k \times n$ . We consider three values for the total computational budget (number of function evaluations):  $10^5, 10^6$ , and  $10^7$ . The higher budget should directly result in a more accurate estimation. Note though, that since this improvement happens across all models and our main goal is to compare relative performance, we do not consider more budget levels. Further, observe that the tail parameter  $\alpha$  is closely connected to the total budget (the higher the value of  $\alpha$  the fewer observations are included in the tail), and hence varying  $\alpha$  is closely tied to varying the budget.

For each value of the total budget, we consider a variety of possible allocations between the number of design points, observations, and replications, as given in Table 3. The higher the value of each of the parameters, the more accurate the resulting model. On the other hand, since the three are constrained by the total budget, it may be interesting to evaluate which combination renders the best performance. Further, we expect that there may be a difference in the relative performance of the different models for different combinations. Consequently, in the remainder of this section, when discussing the results, we both compare all cases for each of the three budgets and analyze the relative performance between different models within each case.

The cases with  $n = 1$  are designed to evaluate the performance of the meta-model where the intrinsic variance is estimated using one replication only. This shows the potential improvement of assigning all the budget to the observations (i.e. estimating CVaR once), instead of replicating the CVaR estimate  $n$  times and consequently estimating the empirical variance using equation (11).

In the second set of experiments we evaluate our method with a simple Stochastic Activity Network (SAN) considered by Chen, Kim (2016). Five activities are involved in the completion of a project. The time to finish activity  $i$  is denoted by  $T_i$  and follows an exponential distribution. The activity times  $T_i$  are assumed to be i.i.d of the other activity times.  $T_3$  follows an exponential distribution with mean  $x \in [0.3, 2]$ , while for any  $i \neq 3$ ,  $T_i$  is exponentially distributed with mean 1. In this network, three paths are defined. The project completion time is specified as follows:

$$L(x) = \max\{T_1 + T_2, T_1 + T_3(x), T_4 + T_5\}$$

We are then interested in estimating CVaR as a function of  $x$ . The experimental design space for the mean parameter  $x$  is  $x \in [0.3, 2]$ . Seven equally spaced design points are chosen from the design space. At each design point,  $N$  observations are simulated. Based on these observations, CVaR and its variance are estimated.

Choosing an appropriate spatial correlation function is one of the most important steps in Gaussian processes. In this study a Gaussian correlation function is used, given by

$$r(x - x', \theta) = \exp\left(-\sum_i \theta_i (x_i - x'_i)^2\right)$$

Table 3: Budget breakdown and test cases for the set of experiments with benchmark function

Budget Identifier	Number of design points ( $k$ )	Number of replications ( $n$ )	Number of Observations ( $N$ )	Total Budget
1	50	10	200	100,000
2	50	5	400	
3	50	1	2000	
4	100	5	200	
5	100	1	1000	
6	50	20	1000	1,000,000
7	50	10	2000	
8	100	10	1000	
9	100	5	2000	
10	100	1	10,000	
11	50	100	2000	10,000,000
12	100	50	2000	
13	100	10	10,000	
14	100	5	20,000	
15	100	1	100,000	

where  $\theta_i$  determines how quickly the spatial correlation decays as the two points become farther apart in each dimension  $i$ . Finding a well-specified polynomial trend can be burdensome and might result in the ill-specification of the model as the test function is designed to have many oscillations. Therefore, Stochastic kriging is performed with  $f(x)^T \beta = \beta_0$  which is widely used in practice due to its simplicity. However, it is worth noting that SK without the trend terms can still lead to good predictions if the kernel and its parameters are well-estimated.

The design points are selected with a Latin hypercube sampling (LHS) procedure, one form of stratified sampling to generate a near-random sample of parameter values in a multidimensional domain. In the one-dimensional case, the CDF is divided into  $n$  equal partitions, and a random point is sampled from each partition. In the multidimensional case, a one-dimensional LHS sample is drawn for each dimension, which is then combined randomly. This design is often used to construct computer experiments to reduce computational effort. Theoretical results demonstrate that LHS shows favorable performance, even in multidimensional cases, see for example, J. C. Helton, F. J. Davis (2003)

Mean Average Percentage Error (MAPE) is used to evaluate the performance of the surrogate models. In order to draw fair comparisons between the different noise distributions, as well as between different simulation budgets/cases, we evaluate and test the metamodels constructed for each budget over the same test set which is sampled using LHS across the domain, independently from the set of design points.

To assess the performance of our proposed method denoted by POT-EVT (i.e., POT estimate of CVaR and EVT estimate of its variance), the results of three other approaches are used as benchmarks.

- Ordinary kriging where we ignore the intrinsic noise in the estimations of CVaR. As was expected, in the cases where the number of observations is relatively large, the estimate of CVaR becomes very accurate (i.e. very close to the true CVaR) and therefore, the ordinary kriging performs as well as the other methods. This method is labeled as ORD-KRG.
- A global SK with POT estimate of CVaR and intrinsic variance as the expectation of the squared deviation of CVaR estimates (11) at each design point. This method builds on the previous approach outlined in Kennedy et al. (2020) and is denoted by POT-EMP in our results (i.e., POT CVaR estimation with the empirical estimation of variance).
- An SK model with empirical estimates of both CVaR and its variance. Note that this method was considered by Chen, Kim (2016). The variance of CVaR is estimated based on (14). This method is denoted by EMP-EMP in our results.

Note that EMP-EMP and our proposed approach, POT-EVT, only require  $n = 1$ . For the cases with the number of replications,  $n$ , greater than 1, each associated replication with a given design point would have its own variance estimate. The mean and variance of the sample mean,  $\bar{Y}$ , are used to construct the kriging models. That is, at each design point, the mean of CVaR estimations,  $\hat{E}(\bar{Y})$ , and the variance of the mean,  $\hat{Var}(\bar{Y})$  (equations (24), (25) respectively) are used as the replications are independent of one another, i.e.,

$$\hat{E}(\bar{Y}) = \frac{CVaR_1 + CVaR_2 + \dots + CVaR_n}{n} \quad (24)$$

$$\hat{Var}(\bar{Y}) = \frac{Var(CVaR_1)}{n^2} + \frac{Var(CVaR_2)}{n^2} + \dots + \frac{Var(CVaR_n)}{n^2} \quad (25)$$

Each combination of the budget allocation ( $k - n - N$ ) is replicated 10 times and the median of the performance of the constructed kriging models is reported in the results section.

## 4.2 Experimental Results

### 4.2.1 Benchmark function

Tables 4–7, and Figures 2–4 summarise the results for the first set of experiments with the benchmark function. Specifically, Tables 4–6 report the median MAPE for the four methods across the three budget levels. The same data is depicted in Figures 2–4 as boxplots (based on the 10 replications of the estimates). Note that here we only present the case of  $\alpha = 0.99$ , while the rest are given in the Appendix. Finally, Table 7 shows the results of the Wilcoxon Signed Rank test for the difference between our proposed and the EMP-EMP method.

Overall, for triangular noise, methods show similar performance, especially with larger budgets. This is expected as the triangular distribution is bounded, and with enough observations, all methods converge to estimates with low error. Additionally, our methodology is best suited for Pareto noise due to its heavy-tailed nature, which concentrates risk in the distribution tail, making accurate estimation crucial. Notably, ordinary kriging is not competitive with lower budgets (higher  $\alpha$ ), so we do not discuss it in detail below.

As can be expected, the surrogate model fitted with a higher number of design points performs better across the different noise distributions. Table 4 shows the results of the test function with the three different additive noises for three different  $\alpha$  levels. As expected, in the cases with 100 design points, the MAPE measures are relatively small especially for the normal and triangular noise, since the CVaR estimates at each design point are very close to the true CVaR due to the limited tail of distributions. In almost all cases, the models that take into account intrinsic variance outperform the ordinary kriging. Note that the trials with one replication (i.e.  $n = 1$ ) assign all of the computational budgets to CVaR estimation, therefore the CVaR estimates are very accurate.

At each budget level ( $10^5$ ,  $10^6$ , and  $10^7$ ), comparing different trials reveals the trade-off between design points, replications, and observations. For example, comparing 100-1-1000 and 100-5-200 demonstrates that one replication with more observations yields slightly better models than five replications with fewer observations. This suggests that using our proposed method, POT-EVT, or the EMP-EMP method, which estimates CVaR variance based on a single replication, outperforms allocating part of the simulation budget to replicate CVaR estimation for intrinsic variance calculation.

Due to the heavy-tailed nature of the Pareto distribution, CVaR estimates are less accurate compared to other additive noise distributions. Consequently, this leads to a larger deviation from the true CVaR and a higher MAPE when compared to normal noise. As anticipated, when using an  $\alpha$  level of 0.95, CVaR estimations become relatively more accurate, thanks to a larger number of observed exceedances over the value at risk. This results in smaller variance in CVaR estimations, improving the overall prediction of CVaR at this  $\alpha$  level and budget.

Table 4: Median of 10 MAPEs for predicting CVaR with a total budget of  $10^5$ . Note that the second row of the table corresponds to the confidence level of the  $CVaR_\alpha$  and the budget column shows the budget breakdown ( $k - n - N$ ) and the number beneath it corresponds to the budget identifier from table 3

Method	Budget*	Normal			Pareto			Triangular		
		0.95	0.99	0.995	0.95	0.99	0.995	0.95	0.99	0.995
ORD-KRG	50-10-200 1	21.06	14.48	13.89	42.39	125.73	146.70	28.68	24.52	23.83
POT-EMP		17.28	13.44	15.08	8.18	23.43	27.27	41.43	19.37	18.82
EMP-EMP		17.47	13.46	14.78	8.10	23.01	36.54	31.66	19.31	18.77
POT-EVT		17.15	13	14.35	15.56	29.92	34.08	22.79	19.25	18.82
ORD-KRG	50-5-400 2	20.99	14.14	13.10	35.02	69.37	71.68	28.75	24.65	23.86
POT-EMP		17.02	12.63	11.75	7.75	16.53	21.80	41.52	19.4	18.84
EMP-EMP		17.08	12.66	11.94	7.64	22.46	30.42	41.47	19.44	18.82
POT-EVT		17.14	12.38	11.49	10.90	21.88	28.43	21.89	19.29	18.81
ORD-KRG	50-1-2000 3	21.11	14.10	12.88	10.91	16.91	21.31	28.76	24.69	23.95
POT-EMP		-	-	-	-	-	-	-	-	-
EMP-EMP		17.14	12.57	11.64	8.58	21.80	28.72	41.65	19.43	18.93
POT-EVT		17.05	12.39	12.05	8.29	17.64	23.66	21.87	19.41	18.89
ORD-KRG	100-5-200 4	7.38	9.27	10.65	49.42	99.78	158.97	3.79	3.91	4.19
POT-EMP		6.29	8.27	10.32	10.46	23.66	33.22	3.40	3.66	4
EMP-EMP		6.7	8.75	10.53	11.40	30.56	41.84	3.33	3.50	3.53
POT-EVT		5.77	8.1	9.83	14.29	32.69	41.76	6.88	3.92	4.22
ORD-KRG	100-1-1000 5	6.79	7.59	8.5	15.98	26.55	30.81	3.64	3.39	3.44
POT-EMP		-	-	-	-	-	-	-	-	-
EMP-EMP		5.88	6.07	7.26	10.24	26.40	36.13	3.34	3.20	3.13
POT-EVT		6.29	6.64	7.55	10.78	24.96	31.93	3.50	3.21	3.20

Table 5: Median of 10 MAPEs for predicting CVaR with a total budget of  $10^6$ 

Method	Budget	Normal			Pareto			Triangular		
		0.95	0.99	0.995	0.95	0.99	0.995	0.95	0.99	0.995
ORD-KRG	50-20-1000 6	21.04	13.87	12.33	7.61	14.52	19.43	28.73	24.71	23.94
POT-EMP		16.94	11.97	10.81	5.24	5.73	15.65	41.50	19.36	18.86
EMP-EMP		16.96	12.13	10.86	4.73	11.33	13.41	41.45	19.38	18.88
POT-EVT		16.98	11.96	10.77	5.04	5.38	14.27	21.84	19.36	18.86
ORD-KRG	50-10-2000 7	21.07	13.78	12.19	4.40	7.72	10.15	28.76	24.71	23.94
POT-EMP		17.04	11.96	10.88	4.59	4.39	5.09	41.57	19.37	18.90
EMP-EMP		16.97	11.91	10.88	4.64	6.03	12.42	41.53	19.40	18.92
POT-EVT		17.03	11.92	10.74	4.54	4.12	4.52	21.82	19.37	18.90
ORD-KRG	100-10-1000 8	3.68	4.10	4.31	9.77	16.12	24.78	3.05	2.84	2.87
POT-EMP		3.46	4.03	4.30	4.68	4.41	10.24	2.78	2.64	2.67
EMP-EMP		3.54	3.95	4.50	4.65	9.20	14.02	2.82	2.61	2.59
POT-EVT		3.09	3.45	3.49	4.56	4.35	14.69	2.79	2.64	2.68
ORD-KRG	100-5-2000 9	3.23	3.47	3.91	6.13	10.65	13.14	3.04	2.81	2.84
POT-EMP		3.18	3.24	3.63	4.23	4.66	5.17	2.89	2.64	2.66
EMP-EMP		3.22	3.36	3.69	4.80	8.43	17.10	2.84	2.63	2.66
POT-EVT		3.04	2.93	3.29	4.48	4.86	5.00	2.90	2.66	2.68
ORD-KRG	100-1-10,000 10	3.41	3.38	3.93	5.30	8.63	9.97	3.17	2.76	2.80
POT-EMP		-	-	-	-	-	-	-	-	-
EMP-EMP		2.84	2.99	3.32	4.81	7.94	12.63	2.79	2.54	2.64
POT-EVT		3.00	3.11	3.41	4.30	4.86	6.63	2.88	2.57	2.60

Table 6: Median for 10 MAPEs for predicting CVaR with a total budget of  $10^7$ 

Method	Budget	Normal			Pareto			Triangular		
		0.95	0.99	0.995	0.95	0.99	0.995	0.95	0.99	0.995
ORD-KRG	50-100-2000 11	21.05	13.72	12.21	2.84	4.58	5.77	28.76	24.71	23.94
POT-EMP		16.94	11.81	10.78	3.33	3.98	4.73	41.56	19.36	18.87
EMP-EMP		16.93	11.80	10.84	3.34	3.11	3.91	31.67	19.38	18.89
POT-EVT		16.93	11.85	10.72	3.34	3.96	4.72	21.82	19.36	18.87
ORD-KRG	100-50-2000 12	2.54	2.19	2.37	2.82	5.38	7.02	3.00	2.54	2.76
POT-EMP		2.70	2.70	3.10	2.27	3.76	4.33	2.75	2.56	2.54
EMP-EMP		2.73	2.76	3.19	2.01	3.35	4.43	2.75	2.52	2.51
POT-EVT		2.36	2.11	2.34	2.29	3.71	4.23	2.75	2.56	2.54
ORD-KRG	100-10-10,000 13	2.64	2.22	2.23	2.04	3.44	4.12	2.99	2.68	2.74
POT-EMP		2.36	2.18	2.15	1.71	2.59	2.47	2.80	2.53	2.54
EMP-EMP		2.39	2.10	2.23	2.05	3.28	3.84	2.79	2.52	2.51
POT-EVT		2.38	2.02	2.03	1.69	2.40	2.43	2.80	2.54	2.54
ORD-KRG	100-5-20,000 14	2.70	2.37	2.17	2.17	3.96	4.37	3.01	2.59	2.70
POT-EMP		2.42	2.00	2.02	1.65	2.36	2.68	2.78	2.54	2.48
EMP-EMP		2.34	1.96	2.02	1.85	3.18	3.93	2.76	2.49	2.48
POT-EVT		2.47	2.01	1.93	1.59	2.26	2.39	2.78	2.54	2.48
ORD-KRG	100-1-100,000 15	2.63	2.27	2.26	2.05	3.27	4.17	2.94	2.64	2.74
POT-EMP		-	-	-	-	-	-	-	-	-
EMP-EMP		2.41	1.90	1.89	1.99	2.98	3.83	2.79	2.49	2.49
POT-EVT		2.43	2.09	2.14	1.51	2.36	2.39	2.79	2.52	2.47

Table 7: P-value results for the one-sided Wilcoxon Signed Rank Test over the MAPE of the POT-EVT and EMP-EMP SK models. Bolded values support our claim that our model has a lower error, while the underlined values show that the EMP-EMP method achieves a lower error.

Budget	Normal						Pareto						Triangular					
	0.95		0.99		0.995		0.95		0.99		0.995		0.95		0.99		0.995	
	<=	>=	<=	>=	<=	>=	<=	>=	<=	>=	<=	>=	<=	>=	<=	>=	<=	>=
1	0.385	0.652	0.188	0.839	0.065	0.947	1.000	<u>0.001</u>	0.998	<u>0.003</u>	0.571	0.429	0.997	<u>0.005</u>	<b>0.010</b>	0.993	0.500	0.539
2	0.903	0.116	0.500	0.539	<b>0.002</b>	0.999	0.999	<u>0.002</u>	0.539	0.500	<b>0.032</b>	0.976	0.813	0.216	0.348	0.688	0.348	0.688
3	0.500	0.539	0.652	0.385	0.722	0.313	<b>0.024</b>	0.981	<b>0.019</b>	0.986	<b>0.001</b>	1.000	0.423	0.615	0.348	0.688	0.080	0.935
4	<b>0.042</b>	<u>0.968</u>	0.313	0.722	0.188	0.839	1.000	<u>0.001</u>	0.993	<u>0.010</u>	0.539	0.500	1.000	<u>0.001</u>	1.000	<u>0.001</u>	1.000	<u>0.001</u>
5	0.813	0.216	0.754	0.278	0.999	<u>0.002</u>	0.995	<u>0.007</u>	0.188	<u>0.839</u>	<b>0.001</b>	1.000	1.000	<u>0.001</u>	0.539	0.500	0.784	0.246
6	0.947	0.065	<b>0.010</b>	0.993	<b>0.042</b>	0.968	0.986	<u>0.019</u>	<b>0.024</b>	0.981	0.754	0.278	0.862	0.161	<b>0.001</b>	1.000	<b>0.001</b>	1.000
7	0.986	<u>0.019</u>	<b>0.024</b>	0.981	<b>0.024</b>	0.981	0.539	0.500	0.053	0.958	<b>0.003</b>	0.998	0.862	0.161	<b>0.002</b>	0.999	<b>0.001</b>	1.000
8	<b>0.042</b>	<u>0.968</u>	<b>0.024</b>	0.981	<b>0.042</b>	0.968	<b>0.080</b>	0.935	<b>0.042</b>	0.968	0.539	0.500	0.722	0.313	0.947	0.065	1.000	<u>0.001</u>
9	0.246	0.784	0.500	0.539	<b>0.042</b>	0.968	<b>0.001</b>	1.000	<b>0.001</b>	1.000	<b>0.001</b>	1.000	0.976	<u>0.032</u>	0.385	0.652	0.461	0.577
10	0.976	<u>0.032</u>	0.577	0.461	0.976	<u>0.032</u>	<b>0.001</b>	1.000	<b>0.001</b>	1.000	<b>0.001</b>	1.000	0.784	0.246	0.754	0.278	0.577	0.461
11	0.839	0.188	0.161	0.862	<b>0.032</b>	0.976	0.884	0.138	0.995	<u>0.007</u>	0.981	<u>0.024</u>	0.968	<u>0.042</u>	<b>0.001</b>	1.000	<b>0.001</b>	1.000
12	0.615	0.423	0.161	0.862	0.216	0.813	0.997	<u>0.005</u>	0.935	0.080	0.188	0.839	0.615	0.423	1.000	<u>0.001</u>	1.000	<u>0.001</u>
13	0.577	0.461	0.339	0.661	0.055	0.945	<b>0.001</b>	1.000	<b>0.001</b>	1.000	<b>0.001</b>	1.000	0.839	0.188	0.958	0.053	0.986	<u>0.019</u>
14	0.784	0.246	0.278	0.754	0.161	0.862	<b>0.001</b>	1.000	<b>0.001</b>	1.000	<b>0.001</b>	1.000	0.998	<u>0.003</u>	0.947	0.065	0.813	0.216
15	0.524	0.476	0.981	<u>0.024</u>	0.784	0.246	<b>0.001</b>	1.000	<b>0.001</b>	1.000	<b>0.001</b>	1.000	0.722	0.313	0.754	0.278	0.188	0.839

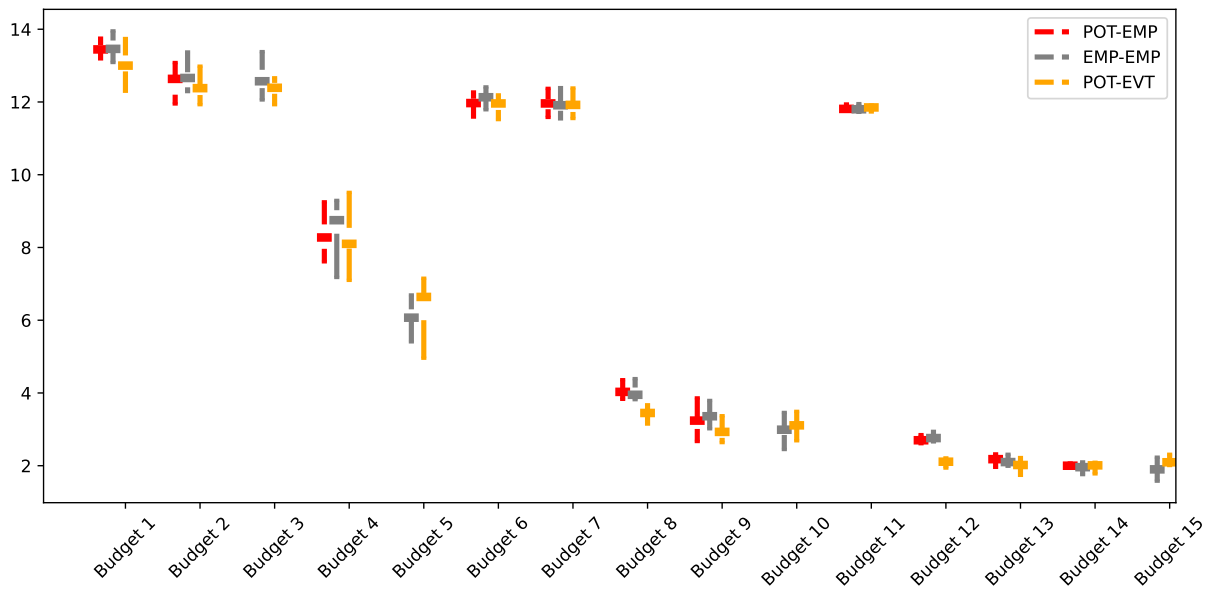


Figure 2: Boxplots for the normal noise  $\alpha = 0.99$

Table 5 shows the results for the test function for the total budget of  $10^6$ . As expected the performance of all the models improved as we increased the total budget. Note that with the triangular noise, the relatively large MAPE measure is due to the small values (close to zero) for the true CVaR. Moreover, since the additive noise term is bounded, the CVaR value can be accurately estimated using both POT and EMP. This results in a lower variance of CVaR and therefore all methods work relatively the same.



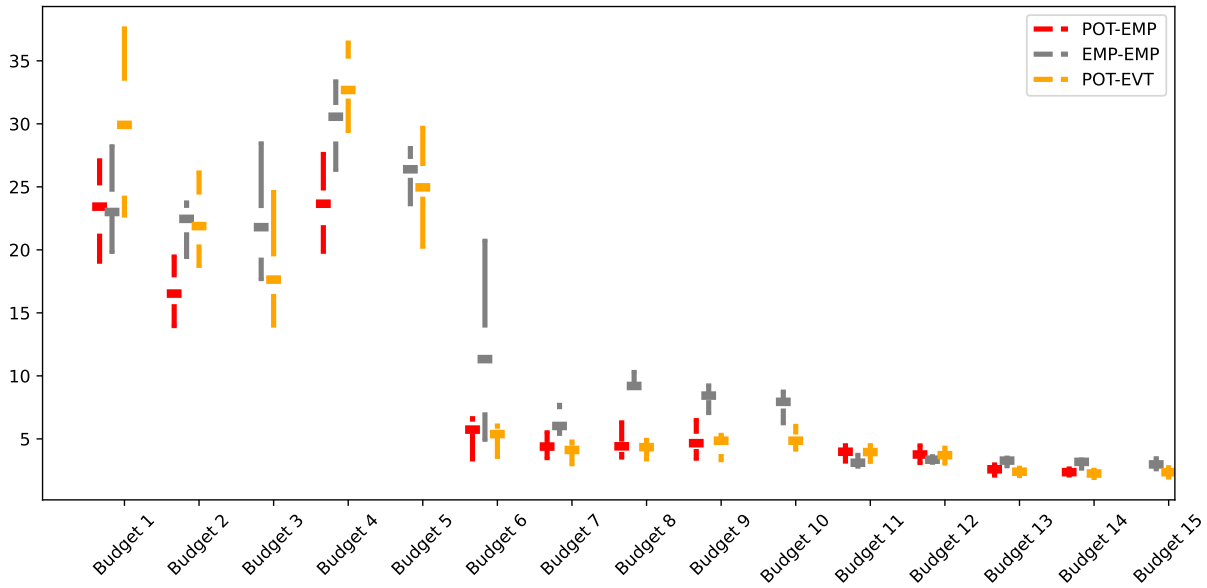


Figure 3: Boxplots for the Pareto noise  $\alpha = 0.99$

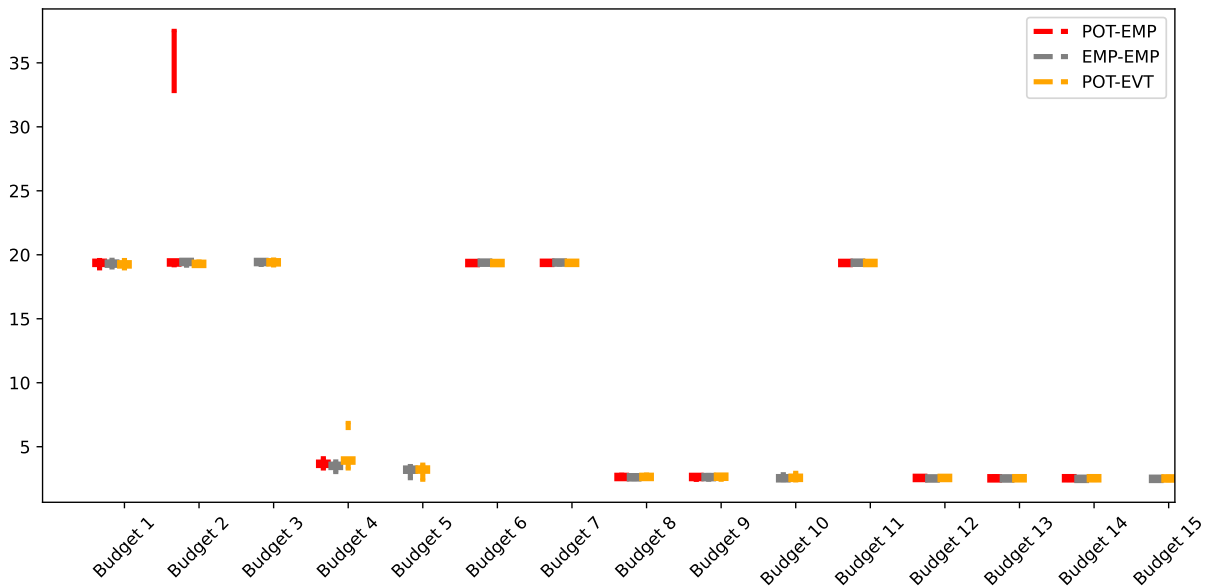


Figure 4: Boxplots for the triangular noise  $\alpha = 0.99$

Table 6 shows the results of the test function for the total budget of  $10^7$ . A relative improvement in performance is observed across all the different method-noise combinations in comparison to the last two tables, as we allocate a larger total budget.

Table 7 displays results from the Wilcoxon Signed Rank test, comparing our method with EMP-EMP. We focus on these two methods as ORD-KRG underperforms, and POT-EMP requires multiple replications at each design point. To assess the relative performance we employ a one-sided hypothesis, rejecting the null hypothesis of a positive median difference at a 5% confidence level. We also consider another one-sided hypothesis favoring EMP-EMP's performance over ours. Bolded values indicate the cases where the proposed approach outperformed EMP-EMP, while underlined values indicate the opposite. In summary, there is a significant number of cases where each methodology is preferred.

Table 8: Median of 10 MAPE measures for predicting CVaR of SAN over the test set

Method	Budget	alpha		
		0.95	0.99	0.995
ORD-KRG	1000	2.59	3.79	4.82
EMP-EMP		1.62	3.32	4.16
POT-EVT		1.65	3.01	4.38
ORD-KRG	10,000	0.65	0.98	1.41
EMP-EMP		0.46	0.75	1.13
POT-EVT		0.39	0.93	1.02
ORD-KRG	100,000	0.25	0.49	0.61
EMP-EMP		0.21	0.39	0.47
POT-EVT		0.24	0.41	0.42

However, EVT-based estimation excels, particularly with larger  $\alpha$  values in the case of Pareto noise (in 9 out of 15 cases and only one opposite result for  $\alpha = 0.995$ ), a crucial scenario due to the potential for significant losses from estimation errors.

#### 4.2.2 Stochastic network experiment

Table 8 shows the results for the SAN problem for three different  $\alpha$  levels, 0.95, 0.99, and 0.995. 193 (resulting in a total of 200, including 7 design points) equally spaced points are chosen from the domain space to evaluate the performance of the surrogate model. The true value of CVaR at each of these design points is obtained numerically by inverting the CDF of the random project time. The obtained MAPE measures for each different  $\alpha$  level are provided as a box plot (Figure 5– 7) to graphically depict groups of MAPE measures through their quartiles.

Table 9: P-value results for the one-sided Wilcoxon Signed Rank Test over the MAPE of the POT-EVT and EMP-EMP SK models. Bolded values support our claim that our model has a lower error, while the underlined values show that EMP-EMP method achieves a lower error.

Budget	$\alpha$					
	0.95		0.99		0.995	
	$\leq$	$\geq$	$\leq$	$\geq$	$\leq$	$\geq$
1000	0.278	0.754	0.539	0.500	0.138	0.884
10000	0.839	0.188	0.385	0.652	0.754	0.278
100000	0.313	0.722	<b>0.032</b>	0.976	0.161	0.862

Table 9 shows the p-values resulting from the one-sided and two-sided Wilcoxon Signed Rank test over the difference of MAPE measure between the POT-EVT method and EMP-EMP method. As shown the two methodologies perform mostly the same because the intrinsic variability of CVaR estimations is relatively small. Also, it can be observed in Table 8 that as the number of observations increases, the performance of the ordinary kriging model (with no intrinsic variance) becomes relatively similar to the other methodologies due to the fact that the variance of the CVaR estimations drops.

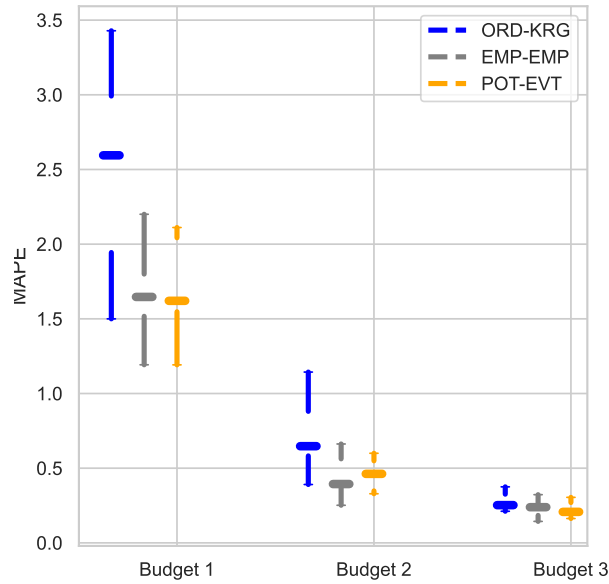


Figure 5: SAN results boxplots for  $(\alpha = 0.95)$

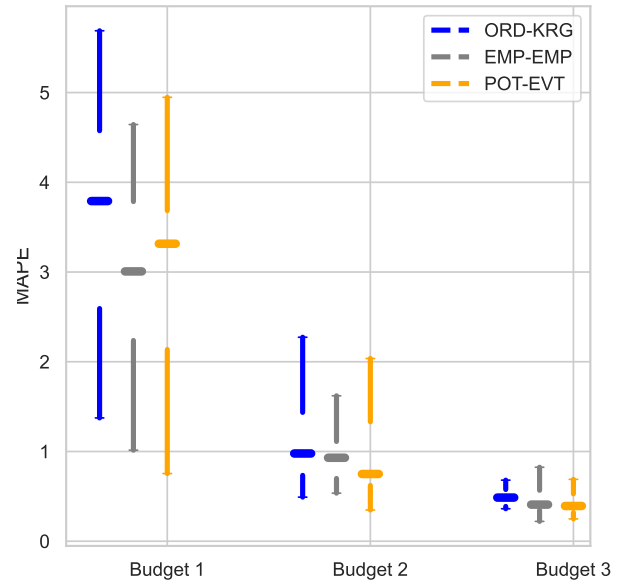


Figure 6: SAN results boxplots for  $(\alpha = 0.99)$

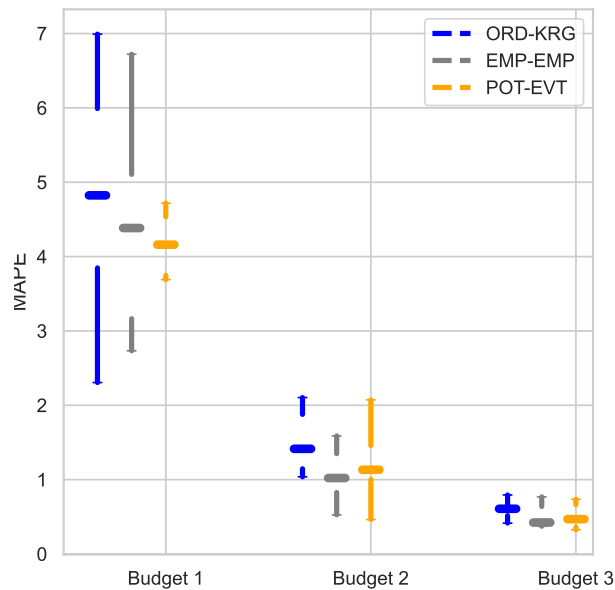


Figure 7: SAN results boxplots for  $(\alpha = 0.995)$

## 5 Conclusions and Future Research

In this work, we investigated the potential of metamodeling combined with extreme value theory to address risk management in simulation models. We used Stochastic kriging to globally characterize tail behavior, and we developed a framework with efficient methods for estimating intrinsic variance without multiple replications. To test and evaluate our proposed method, we used two numerical examples with different budget allocations and noise levels. We compared our proposed methodology with other methods in the literature and generally observed that using POT estimation of CVaR and its approximate asymptotic variance for stochastic spatial functions with a fat-tailed additive noise at high  $\alpha$  levels outperforms the existing empirical approaches.

Although we perform numerical tests under different scenarios with the two benchmark examples, it nevertheless is necessary to validate our methodology with large and complex simulation models of real-world problems. We expect that numerical issues would arise in fitting high-dimensional kriging models. Moreover, we consider stochastic kriging without the trend term. Naturally, in some applications, using a form of polynomial trend term can result in better predictions. While we expect that a similar methodology can be employed in such cases, this is not explicitly tested here. In this work we use MLE to estimate the GPD parameters, however, other estimation methods such as the method of Probability-Weighted Moments and the method of Moments can be useful methods to look into as they are shown to be more reliable with smaller sample size (Hosking, Wallis, 1987).

Lastly, POT is not the only existing approach to evaluating extreme behavior of stochastic systems. Block maxima approach is another popular approach within the general extreme value theory framework. Both block maxima and POT have advantages and disadvantages and are widely used (see, for example, R. S. Tsay, 2005, specifically in the context of risk measurement). A thorough investigation of the potential to employ block maxima for CVaR or other risk measure estimation for metamodelling application is beyond the scope of this study and could be a topic for a future study.

## Supplementary materials

All code required for implementing the proposed method and that was used for the numerical experiments is available at [https://github.com/arminkhayyer/EVT\\_CVaR\\_SK/tree/master](https://github.com/arminkhayyer/EVT_CVaR_SK/tree/master).

## Disclosure statement

All authors certify that they have no affiliations with or involvement in any organization or entity with any financial interest or non-financial interest in the subject matter or materials discussed in this manuscript.

## Funding

Part of this work was funded by the project “SBIR Phase III – Analytical Framework and Modeling to Support Wargaming Logistics” by Frontier Technology, Inc.

## References

- Acerbi Carlo*. Spectral measures of risk: A coherent representation of subjective risk aversion // *Journal of Banking & Finance*. 2002. 26, 7. 1505–1518.
- Ankenman Bruce, Nelson Barry L., Staum Jeremy*. Stochastic Kriging for Simulation Metamodeling // *Operations Research*. 2010. 58, 2. 371–382.
- Asmussen Søren, Glynn Peter W*. Stochastic simulation: algorithms and analysis. 57. 2007.
- Balkema A. A., Haan L. de*. Residual Life Time at Great Age // *The Annals of Probability*. 1974. 2, 5. 792–804.
- Barton Russell R, Meckesheimer Martin*. Metamodel-based simulation optimization // *Handbooks in operations research and management science*. 2006. 13. 535–574.
- Beguiría Santiago, Vicente-Serrano Sergio M*. Mapping the Hazard of Extreme Rainfall by Peaks over Threshold Extreme Value Analysis and Spatial Regression Techniques // *Journal of applied meteorology and climatology*. 2006. 45, 1. 108–124.
- Bracken C, Holman KD, Rajagopalan B, Moradkhani Hamid*. A Bayesian Hierarchical Approach to Multivariate Nonstationary Hydrologic Frequency Analysis // *Water Resources Research*. 2018. 54, 1. 243–255.
- Chen Xi, Kim Kyoung-Kuk*. Efficient VaR and CVaR Measurement via Stochastic Kriging // *INFORMS Journal on Computing*. 2016. 28, 4. 629–644.
- Dabo-Niang Sophie, Thiam Baba*. Robust quantile estimation and prediction for spatial processes // *Statistics & probability letters*. 2010. 80, 17-18. 1447–1458.
- De Haan Laurens, Ferreira Ana, Ferreira Ana*. Extreme value theory: an introduction. 21. 2006.
- Fang Kai-Tai, Li Runze, Sudjianto Agus*. Design and modeling for computer experiments. 2005.

- Helton Jon C, Davis Freddie Joe.* Latin hypercube sampling and the propagation of uncertainty in analyses of complex systems // *Reliability Engineering & System Safety.* 2003. 81, 1. 23–69.
- Hosking Jonathan RM, Wallis James R.* Parameter and Quantile Estimation for the Generalized Pareto Distribution // *Technometrics.* 1987. 29, 3. 339–349.
- Kennedy Joseph J., Khayyer Armin, Vinel Alexander, Smith Alice E.* Efficient Risk Estimation Using Extreme Value Theory and Simulation Metamodeling // *2020 Winter Simulation Conference (WSC).* 2020. 385–396.
- Kim Joseph Hyun Tae, Hardy Mary R.* Quantifying and correcting the bias in estimated risk measures // *ASTIN Bulletin: The Journal of the IAA.* 2007. 37, 2. 365–386.
- Koenker Roger, Hallock Kevin F.* Quantile regression // *Journal of economic perspectives.* 2001. 15, 4. 143–156.
- Krokhmal Pavlo, Zabaranin Michael, Uryasev Stan.* Modeling and Optimization of Risk // *Surveys in Operations Research and Management Science.* 2011. 16, 2. 49 – 66.
- Krokhmal Pavlo A.* Higher moment coherent risk measures // *Quantitative Finance.* 2007. 7, 4. 373–387.
- Kusuoka Shigeo.* On law invariant coherent risk measures // *Advances in mathematical economics.* 2001. 83–95.
- Liu Ming, Staum Jeremy.* Estimating Expected Shortfall with Stochastic Kriging // *Proceedings of the 2009 Winter Simulation Conference (WSC).* 2009. November 29 –December 2, Austin, Texas, 1249–1260.
- McNeil Alexander J.* Estimating the Tails of Loss Severity Distributions Using Extreme Value Theory // *ASTIN Bulletin: The Journal of the IAA.* 1997. 27, 1. 117–137.
- McNeil Alexander J, Saladin Thomas.* The Peaks Over Thresholds Method for Estimating High Quantiles of Loss Distributions // *Proceedings of 28th International ASTIN Colloquium.* 1997. August 10 – 13, Cairns, Australia, 23–43.
- Mitchell Toby, Morris Max, Ylvisaker Donald.* Asymptotically optimum experimental designs for prediction of deterministic functions given derivative information // *Journal of statistical planning and inference.* 1994. 41, 3. 377–389.
- Norton Matthew, Khokhlov Valentyn, Uryasev Stan.* Calculating CVaR and bPOE for Common Probability Distributions with Application to Portfolio Optimization and Density Estimation // *Annals of Operations Research.* X 2019.
- Pickands III James.* Statistical Inference Using Extreme Order Statistics // *The Annals of Statistics.* 1975. 3, 1. 119–131.
- Reza Najafi Mohammad, Moradkhani Hamid.* Analysis of Runoff Extremes Using Spatial Hierarchical Bayesian Modeling // *Water Resources Research.* 2013. 49, 10. 6656–6670.
- Rockafellar R Tyrrell, Uryasev Stanislav.* Optimization of conditional value-at-risk // *Journal of risk.* 2000. 2. 21–42.
- Rockafellar R Tyrrell, Uryasev Stanislav.* Conditional Value-At-Risk for General Loss Distributions // *Journal of Banking & Finance.* 2002. 26, 7. 1443–1471.
- Rougier Jonathan.* Efficient emulators for multivariate deterministic functions // *Journal of Computational and Graphical Statistics.* 2008. 17, 4. 827–843.
- Smith Richard L.* Maximum likelihood estimation in a class of nonregular cases // *Biometrika.* 1985. 72, 1. 67–90.
- Trindade A Alexandre, Uryasev Stan, Shapiro Alexander, Zrazhevsky Grigory.* Financial prediction with constrained tail risk // *Journal of Banking & Finance.* 2007. 31, 11. 3524–3538.
- Troop Dylan, Godin Frédéric, Yu Jia Yuan.* Risk-Averse Action Selection Using Extreme Value Theory Estimates of the CVaR // *arXiv preprint arXiv:1912.01718.* 2019.
- Troop Dylan, Godin Frédéric, Yu Jia Yuan.* Bias-corrected peaks-over-threshold estimation of the CVaR // *Uncertainty in Artificial Intelligence.* 2021. 1809–1818.
- Tsay Ruey S.* Analysis of financial time series. 2005.
- Wang Songhao, Ng Szu Hui.* A joint Gaussian process metamodel to improve quantile predictions // *2017 Winter Simulation Conference (WSC).* 2017. 1891–1902.

## 6 Appendix

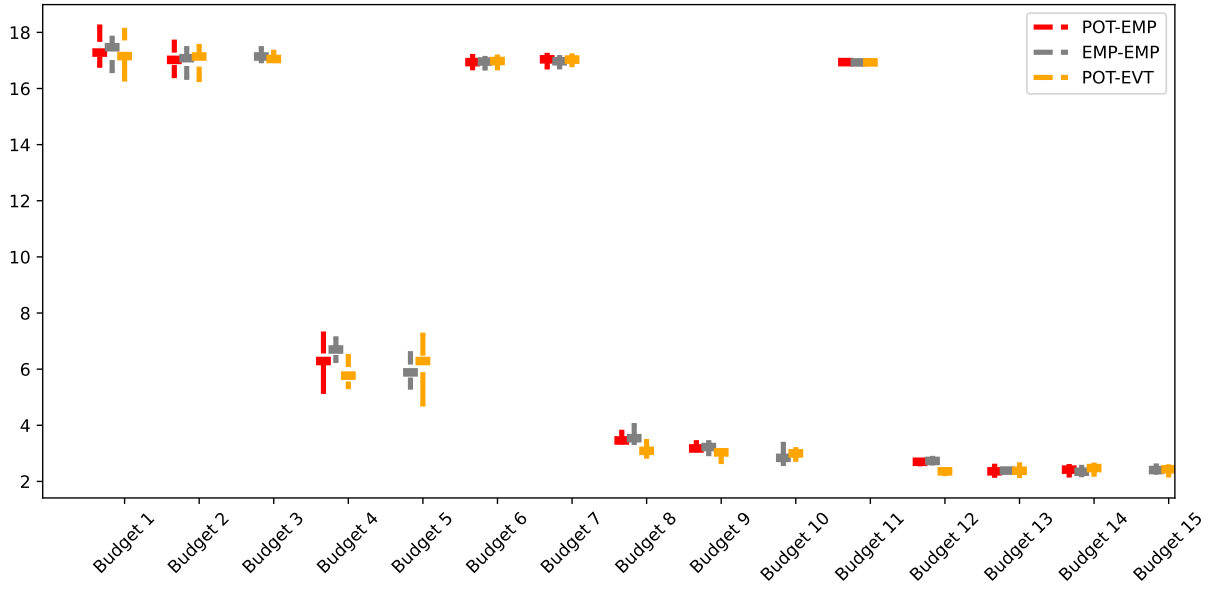


Figure 8: boxplots for the normal noise  $\alpha = 0.95$

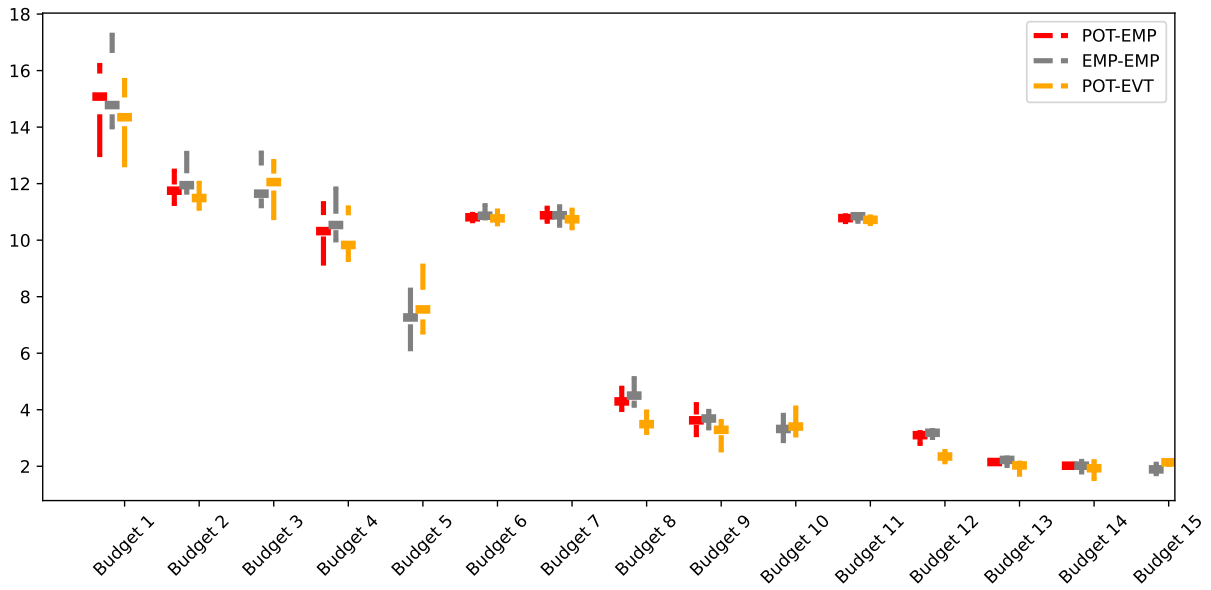


Figure 9: boxplots for the normal noise  $\alpha = 0.995$

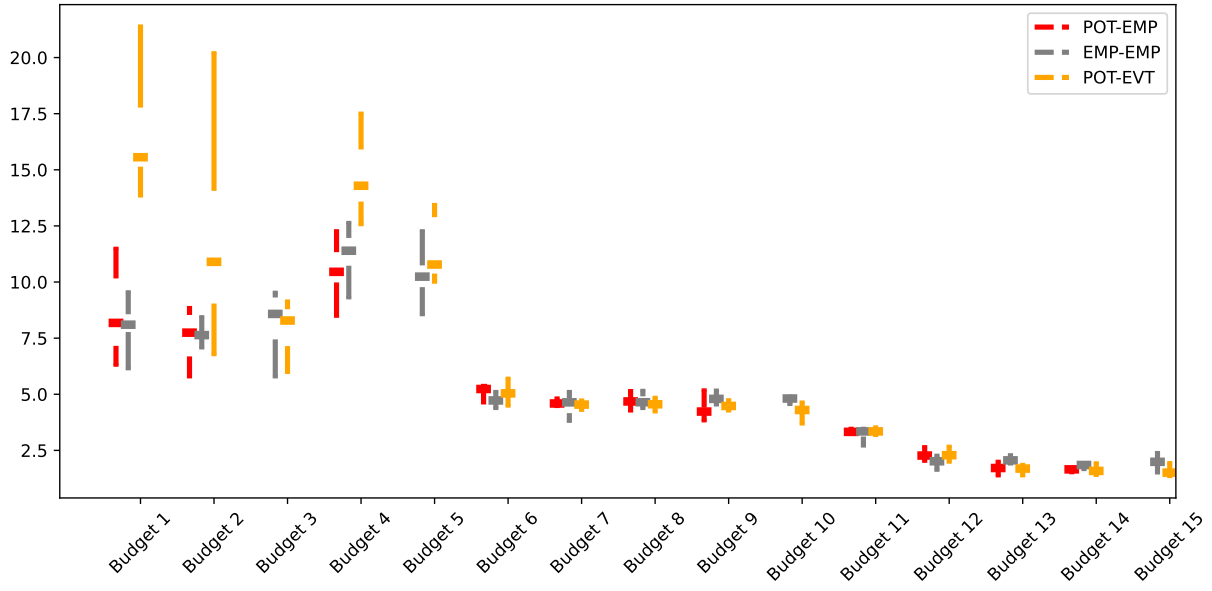


Figure 10: boxplots for the pareto noise  $\alpha = 0.95$

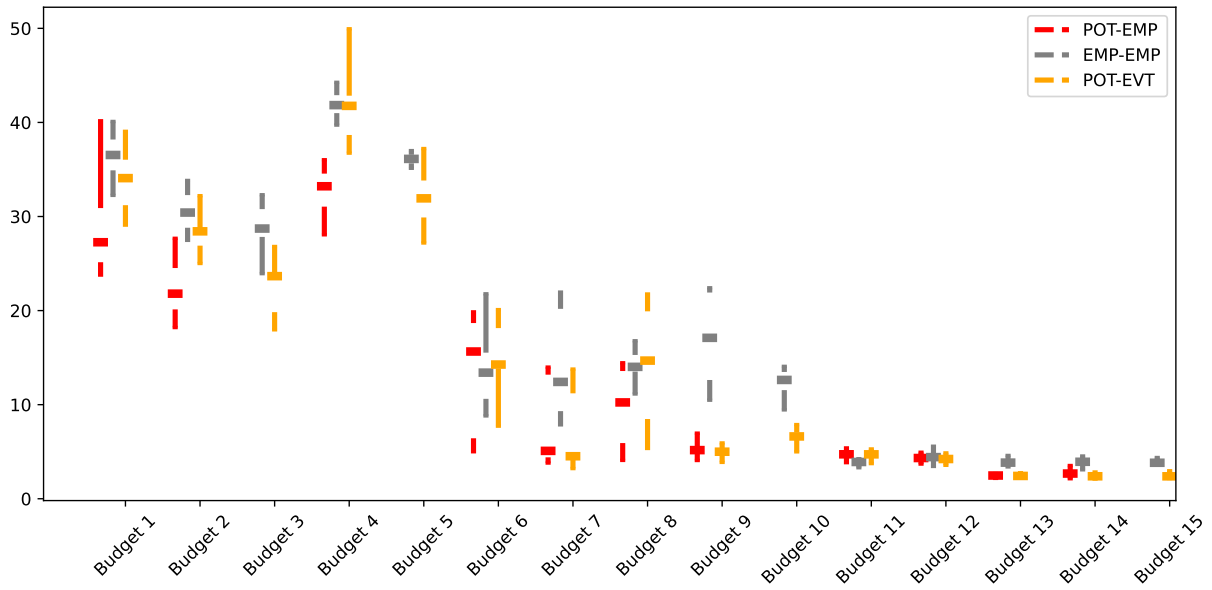


Figure 11: boxplots for the pareto noise  $\alpha = 0.995$

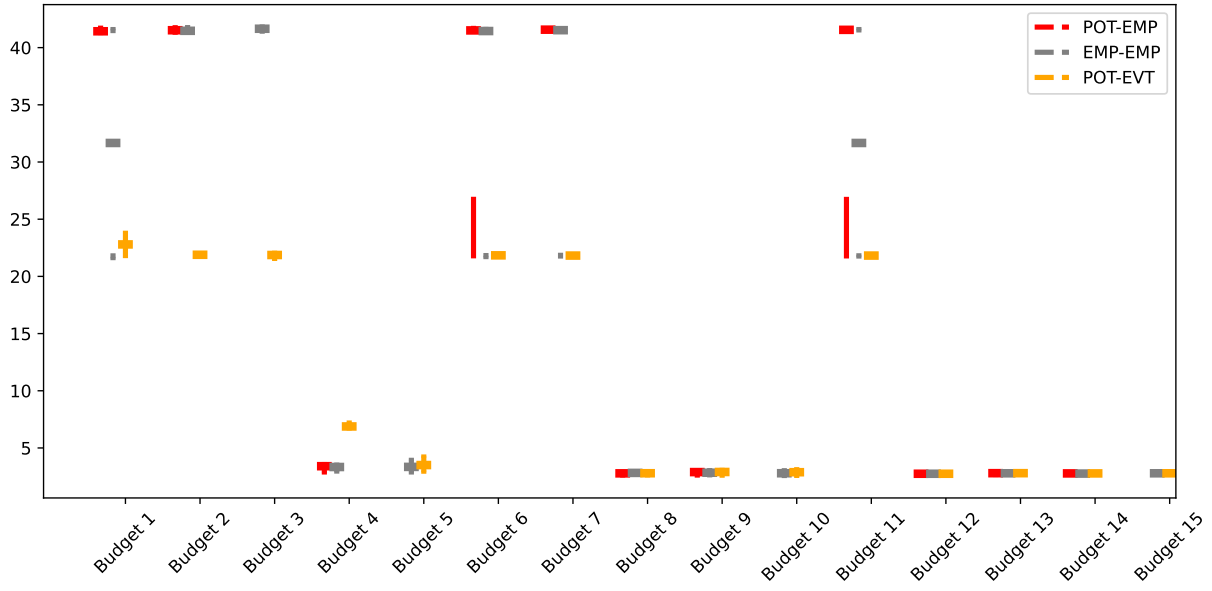


Figure 12: boxplots for the Triangular noise  $\alpha = 0.95$

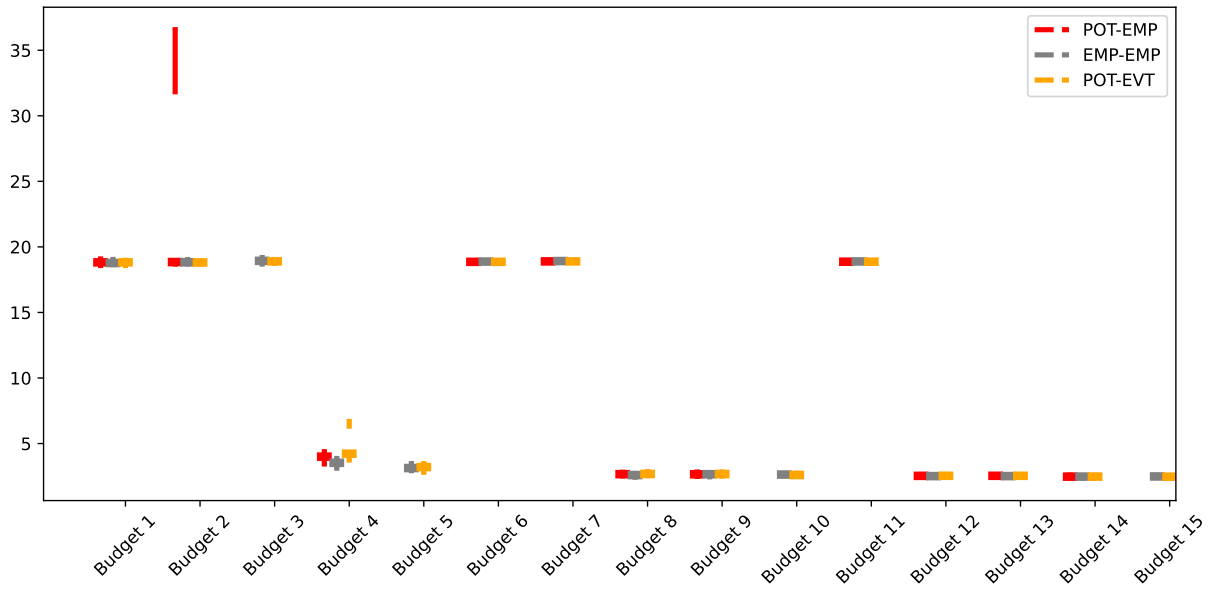


Figure 13: boxplots for the Triangular noise  $\alpha = 0.995$